ChemElectroChem

Research Article
doi.org/10.1002/celc.202400360

Chemistry Europe
European Chemical Societies Publishing

www.chemelectrochem.org

Automated Optimization of the Synthesis of Alkyl Arenesulfonates in an Undivided Electrochemical Flow Cell

Maximilian M. Hielscher[+],[a] Johannes Schneider[+],[a] Alexander H. J. Lohmann,[c] and Siegfried R. Waldvogel*[a, b, c]

The necessary separation of anodic and cathodic compartments in the electrochemical multicomponent synthesis of alkyl arenesulfonates in batch was overcome by the transfer of this reaction in an undivided electrochemical flow cell. The yield was increased from an initial 23% to 67% by optimization using Design of Experiments (DoE). The experiments were carried out using an automated experimental flow electrolysis setup controlled by the automation software LABS (*Laboratory Automation and Batch Scheduling*), an open-source software that allows to plan and conduct experiments with an arbitrary, freely selectable experimental setup. The automated experimental setup turned out to be stable and provides reproducible results. In total, 6 examples are demonstrated with isolated yields up to 81%. In addition, the robust scalability of the electrochemical reaction was demonstrated in a 10-fold scale-up.

Introduction

Organic Electrosynthesis has begun to experience a remarkable and ongoing renaissance, because it offers a variety of advantages over conventional synthetic methods.[1] Electroorganic reactions are typically carried out under mild reaction conditions. Electricity, which can originate from sources of renewable energy, is used as inexpensive and universal redox agent.[2] This allows for innovative electrochemical reaction pathways, which avoid the use of hazardous reagents,[3] and minimize the generation of reagent waste.[4]

In 2020, our group reported the first electrochemical multicomponent synthesis of alkyl arenesulfonates in batch.[5] In this transformation, stock solutions of sulfur dioxide are employed as atom-economic, inexpensive, and simple source of SO_2, entirely avoiding expensive sulfur dioxide surrogates. This work is part of the recent progress in the field of electrochemical incorporation of sulfur dioxide into organic molecules (Figure 1).[6] The electrosynthesis of sulfonates was the basis for following work on the electrosynthesis of sulfonamides,[7] sulfamides,[8] and alkenesulfonates.[9] In addition to the use of SO_2 stock solutions, the synthesis of sulfonamides in flow was demonstrated by the Noël group by an electrochemical coupling between thiols and amines.[10] Previous work by our group used SO_2 multicomponent reactions for the synthesis of sulfonamides in flow by carrying out experiments manually.[11] In recent years however, significant progress was made in automatizing chemical synthesis,[12] often by employing flow chemistry.[13]

Many solutions for laboratory automation require the use of commercial third-party software, or the software which is developed internally is not openly published. In 2022, our group developed *LABS: Laboratory Automation and Batch Scheduling*,[14] a modular, open-source Python based solution. The graphical user interface of the LABS frontend enables the addition of experiments in individual segments, which can then be transferred to the experimental setup. The modular design

[a] *M. M. Hielscher,[+] J. Schneider,[+] Prof. Dr. S. R. Waldvogel*
Department of Chemistry
Johannes Gutenberg University Mainz
Duesbergweg 10–14, 55128 Mainz (Germany)

[b] *Prof. Dr. S. R. Waldvogel*
Institute of Biological and Chemical Systems – Functional Molecular Systems (IBCS-FMS)
Karlsruhe Institute of Technology (KIT)
Kaiserstraße 12, 76131 Karlsruhe (Germany)

[c] *A. H. J. Lohmann, Prof. Dr. S. R. Waldvogel*
Max-Planck-Institute for Chemical Energy Conversion
Stiftstraße 34–36, 45470 Mülheim an der Ruhr (Germany)
E-mail: siegfried.waldvogel@cec.mpg.de

[+] *These authors contributed equally.*

Supporting information for this article is available on the WWW under https://doi.org/10.1002/celc.202400360

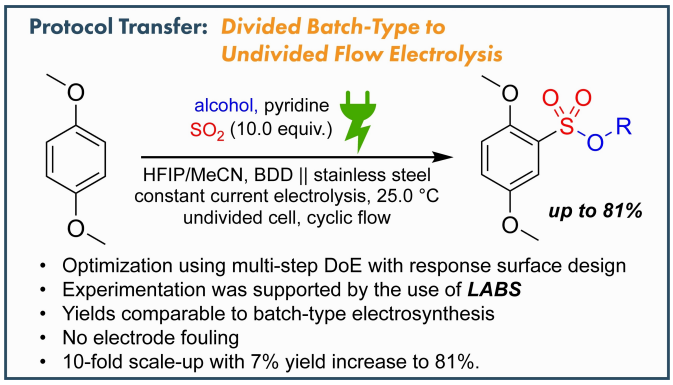

Figure 1. The combination of LABS (Laboratory Automation and Batch Scheduling) and a multi-step DoE-based optimization allowed the transfer of reaction conditions from divided batch to undivided flow without loss of yield.

allows for the automation of any combination of devices by adapting the configuration file. If the device drivers are already available in the LABS repository, no programming knowledge is required on the part of the user to realize these implementations. The flexible architecture allows for the rapid modification of this automated setup, thereby facilitating the user's ability to readily accommodate specific requirements to the test setup.

Here, the study demonstrates the adaptation and utilization of LABS for the automated electrochemical synthesis of sulfonates in flow. To this end, the handling of stock solutions of SO_2 was incorporated into the automation configuration. The electrolysis flow cells utilized as part of the experimental framework presented in this work were devised within our research group and are commercially available.[15] Previously, we employed peristaltic pumps, which revealed that the stability of the tubing rapidly deteriorates due to the high load during electrolysis and rinsing sequences. This results in inconsistent flow rates. We therefore equipped our experimental setup with two piston pumps from *Eldex*. These were integrated into LABS with a corresponding driver file. Design of Experiments (DoE) was used as key technique for the systematic analysis and optimization of the reaction conditions.[16]

Results and Discussion

To transfer the original protocol, which described the conversion in a divided batch cell to flow, several reactions with different settings of the continuous parameters were first carried out without automation (Table S3 in the Supporting Information). The initial maximum yield in a single-pass undivided flow cell was 22%, whereas alterations in the reaction conditions resulted in a 13% decrease in yield.

This prompted us to transfer the whole system to a LABS-controlled setup. To this end, the modified setup was first calibrated regarding the stability of the dosed volumes and the stability of the electrolysis in the operating range of the applied flow rates. Further preliminary experiments have shown that cyclic electrolysis with a reservoir gives better yields than single-pass electrolysis. In this study, the flow rate is always expressed as a multiple of the flow rate required for a single pass (flow multiplier).

An initial 2^{5-1} design showed strong main effects after the first run with higher yields at the respective low (−) parameter settings (Figure 2). A reproduction for a significance-based evaluation of the effects was dispensed with and the parameter range of the optimization was shifted to lower parameter levels. The analysis of the yield in the second design showed a curvature of the response space. Due to physical limitations, the model was extended to a response surface model using a face-centered central composite design (CCD) instead of an orthogonal CCD. The determination of the yield by qNMR permitted the simultaneous measurement of the conversion and selectivity based on the yield of **1**. The corresponding models were analyzed according to the same protocol to verify the plausibility of the data for the yield.

Automated Flow Setup

The principal advancement in comparison to our previous work using LABS is the utilization of piston pumps in combination with peristaltic pumps for procedures requiring high precision and durability. One piston pump is employed to prepare the electrolyte at the beginning of each experiment, while a second piston pump is utilized to pump the electrolyte through the flow-through electrolysis cell (Figure 3).

As the piston pumps are unable to self-prime, an additional peristaltic pump was employed to flush the reservoir residue-free in the cleaning procedure. The vessel for the SO_2 stock solution was cooled to 0 °C separately to ensure concentration stability over the duration of the experiment (Figure 4). The LABS method for cyclic flow electrolysis entails the dosing of reagents in the reservoir, the filling of the electrolysis flow cell with electrolyte solution, and the initiation of cyclic flow electrolysis. Upon completion of the electrolysis process, the reaction solution is pumped to the fraction collector, including additional rinsing with acetonitrile. As a cleaning step, the entire system is flushed first with acetone and then with

1 Initial 2^{5-1} Design

Parameter (unit)	Low (–)	High (+)	Effect (p value)
j (mA/cm²)	15	25	n.d.
Q (*F*)	5	7	n.d.
eq. EtOH	4	6	n.d.
eq. pyridine	4	8	n.d.

A reliable assessment via ANOVA and regression was not feasible due to the parameter range shifting after a single design run as a consequence of low yield.

2 Second 2^{5-1} Design

Parameter (unit)	Low (–)	High (+)	Effect (p value)
j (mA/cm²)	10	20	-7% (>0.001)
Q (*F*)	4	6	-2% (0.096)
eq. EtOH	3	5	-6% (>0.001)
eq. pyridine	3	5	+5% (>0.001)
vol.% HFIP	40	60	-10% (>0.001)

Backward elimination for yield ($p > \alpha = 0.1$) | R^2 = 91% | mean yield (qNMR) = 56% | *p*(curvature) = >0.001 | six significant two factor interaction found.

3 Face Centerd CCD

Parameter (unit)	Low (–)	High (+)	Effect (p value)
j (mA/cm²)	10	20	-4% (>0.001)
Q (*F*)[a]	4	6	-1% (0.150)
QQ (*F*)[a]	4	6	-5% (0.001)
eq. EtOH[a]	3	5	-3% (>0.001)
eq. pyridine	3	5	+2% (>0.001)
vol.% HFIP[a]	40	60	-5% (>0.001)

Backward elimination for yield ($p > \alpha = 0.1$) | R^2 = 86% | mean yield (qNMR) = 62% | six significant two factor interaction found | [a] A quadratic response is observed in *vol.% HFIP*, *Q* and *eq. EtOH*.

Figure 2. Optimization strategy for the yield. The same modeling via regression and analysis of variance (ANOVA) was also done for the system responses conversion and selectivity. HFIP = 1,1,1,3,3,3-hexafluoro-2-propanol. CCD = Central Composite Design.

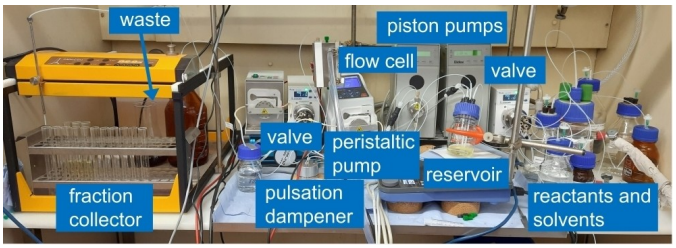

Figure 3. Photograph of the automated electrolysis setup. The reactants are held in screw-cap glass bottles (right). The electrolyte is prepared in the reservoir with stirring (center). The valve downstream of the electrolysis cell allows the electrolyte to be returned to the reservoir, to the fraction collector, or the waste. Picture by A. H. J. Lohmann.

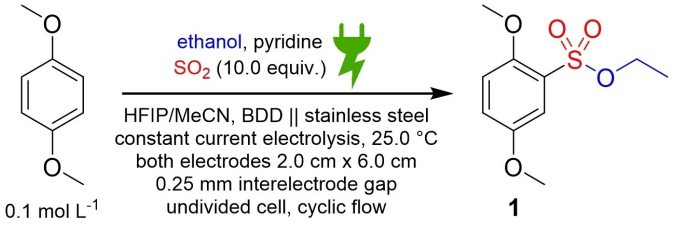

Scheme 1. Electrochemical multi-component synthesis of ethyl 2,5-dimethoxy-benzenesulfonate (**1**) directly from 1,4-dimethoxybenzene, SO_2, and ethanol in an undivided flow electrolysis cell.

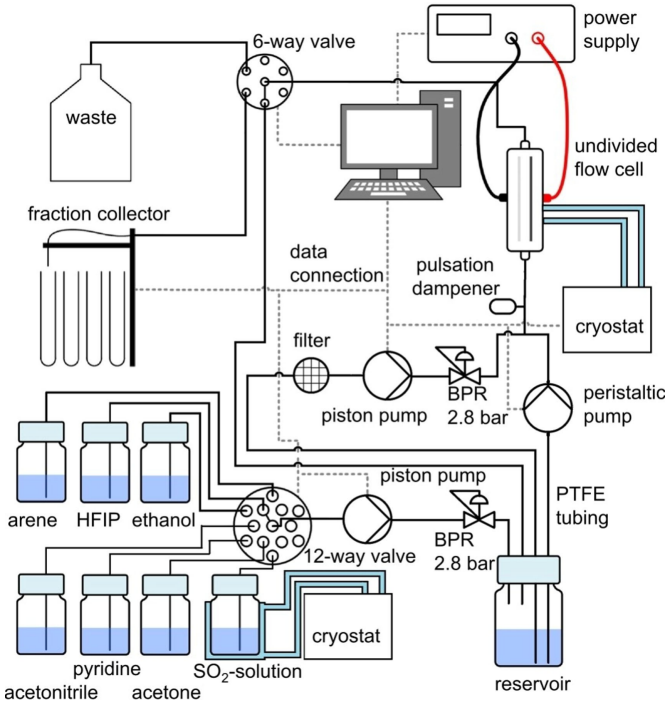

Figure 4. Flow diagram of the electrolysis setup. BPR: back pressure regulator.

acetonitrile. Further details on the experimental setup can be found in the Supporting Information.

Investigation of Flow Multiplier and System Stability

First, the influence of the flow multiplier for the cyclic flow mode was analyzed in relation to the flow rate required for single-pass electrolysis. The resulting higher flow rates can have a positive effect on mass transport to and from the interface. However, to apply the necessary charge, the solution must either be pumped through the cell several times from one reservoir or a cascade mode with a second reservoir must be chosen.[17] Due to the simpler implementation, we have decided in favor of the first case (Scheme 1).[18] To investigate which flow multiplier to use, the reaction was carried out in duplicates with flow multipliers ranging from 1 to 5 in steps of 1 (Table S4 in the SI).

For all subsequent experiments, we have chosen a flow multiplier of 5 to ensure a sufficient passing rate of the total electrolyte. Moreover, the single-pass experiments at the beginning of the study yielded 22–23% at high current densities of 25 mA cm^{-2}, whereas experiments with lower current densities and thus lower flow rates yielded poorer yields. This could be indicative of a positive influence of improved mass transport.[19] To demonstrate the reproducibility of the electrolysis sequence conducted by the automated experimental setup, the reaction depicted in Scheme 2 was carried out 10 times consecutively with flow multiplier 5.

The NMR yield of **1** was determined to be 53(±3)%. The conversion was found to be 90(±4)%, and the selectivity was determined to be 59(±3)% (Table S5 in the SI). In Figure 5, the results of the flow multiplier screening and the system stability analysis are combined in one graph (the data for this plot can be found in Table S4 and Table S5 in the SI). Following the completion of the final electrolysis and clean-up program, the flow cell was disassembled, and no evidence of electrode fouling was observed, which can appear with electron-rich arenes in anodic processes.[20]

Initial Fractional Factorial Design

Based on our initial investigations we included the following five continuous parameters for the DoE-based investigation: the amount of applied charge *Q*, the current density *j*, the equivalents of ethanol and of pyridine, and the amount of HFIP

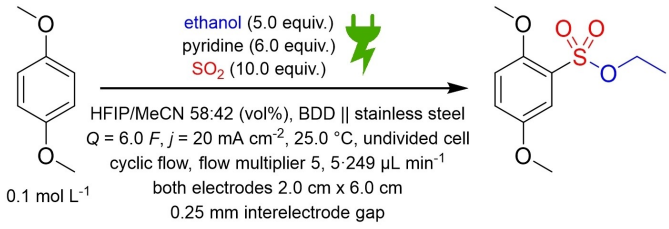

Scheme 2. Reaction conditions for the stability test. The yield, conversion, and selectivity (=yield / conversion) for each of the 10 runs was analyzed using quantitative ^{1}H NMR spectroscopy with 1,3,5-trimethoxybenzene as internal standard.

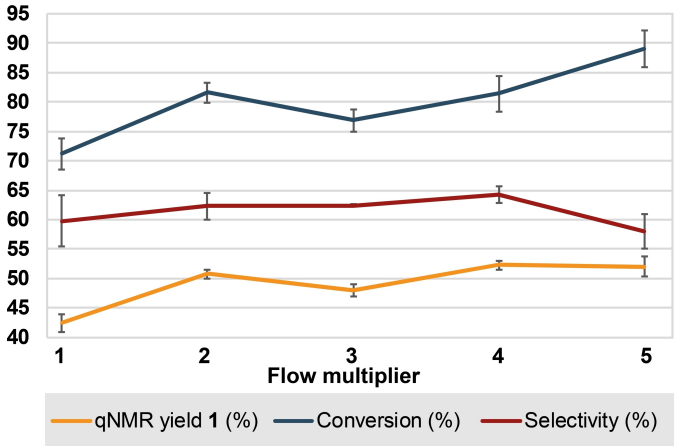

Figure 5. Flow multiplier screening and analysis of system stability. Plot of qNMR yield of **1**, conversion, and selectivity (= yield / conversion) with 1,3,5-trimethoxybenzene as internal standard. For flow multipliers 1 to 4, two runs are shown. 11 runs are shown for flow multiplier 5 (see Table S4 and S5 in the Supporting Information).

in the reaction solution. HFIP plays a key role in this reaction as hydrogen bond donor (see mechanism section in the SI).[21] The following parameters were kept constant: electrode materials (BDD||stainless-steel), interelectrode gap (0.25 mm), temperature of the cathode (25.0 °C), concentration of the starting material in the reaction solution (0.1 mol L^{-1}), equivalents of SO_2 (10.0 equiv.), cyclic flow mode (flow multiplier 5). BDD was chosen as metal-free, electrochemically stable anode material.[22] Using this range of values for the parameters, a 2^{5-1} fractional factorial design without replication was chosen for initial experiments. The yield, conversion, and selectivity (=yield/conversion) were determined using quantitative ^{1}H NMR spectroscopy with 1,3,5-trimethoxybenzene as internal standard. This was maintained for all subsequent optimization experiments to ensure comparability of the measured values. Each experiment required for the initial experimental design was first performed once and the experimental design was analyzed without replication (Figure 2 left). The analysis showed that the selected parameter range was far from the optimum for the reaction (see Table S6 in the SI). We therefore dispensed with further replication and adjusted the parameter limits for a follow-up design. Experiments with upper limit of current density of 25 mA cm^{-2} or amount of applied charge of 7.0 *F* showed poorer yields. We therefore adjusted the parameter range accordingly.

Second Fractional Factorial Design

The results of the first experimental design (Table S6 in the SI) indicated that a shift in the parameter limits of the design was necessary to further enhance the yield (Figure 2 middle). Consequently, the adapted 2^{5-1} design with resolution V was run in duplicate at the corner points for a total of 32 experiments. The central point was systematically run after every fifth experiment to monitor system stability over the course of the campaign. The corner points were executed in randomized order. The results are listed in Table S7 in the Supporting Information. After execution of the experiments and analytics, non-significant terms were excluded from the model using backward elimination ($p < \alpha = 0.1$). The analysis of variance (ANOVA) for the system response yield resulted in a significant *p* value for curvature in the model ($p < 0.001$).[23] To check for nonlinear behaviour within the parameter range of the model, we added star points to achieve a central composite design (CCD). Given that an optimal α-distance for the star points would have resulted in runs that were not feasible due to physical limitations, a non-orthogonal, face-centered CCD was selected as the optimal solution. An orthogonal CCD would have necessitated a range for the HFIP volume percentage that is not attainable without either diluting the starting material in the reaction solution or decreasing the SO_2 equivalents. Furthermore, it is challenging to pump SO_2 stock solutions with concentrations greater than 2.0 mol L^{-1} without loss of SO_2 due to degassing.

Extension to a Central Composite Design

The analysis of the CCD (second FFD including the surface-centered star points, Table S8 in the SI) is carried out analogously using backward elimination ($p < \alpha = 0.1$; Figure 2 right). As previously indicated in the ANOVA of the FFD, the main effect analysis of the CCD reveals the presence of several quadratic terms that contribute significantly to the model of the yield. These terms are primarily associated with the amount of applied charge and the volume fraction of HFIP in the electrolyte (Figure 6). The yield model shows a robust R^2 of 87 %. However, the evaluation using cross-validation reveals a $R^2_{predicted}$ of 75 % indicating a slight overfitting of the model, which may be due to a more complex response surface of the reactions true functional. This evidence holds true for the models based on conversion and selectivity as well.

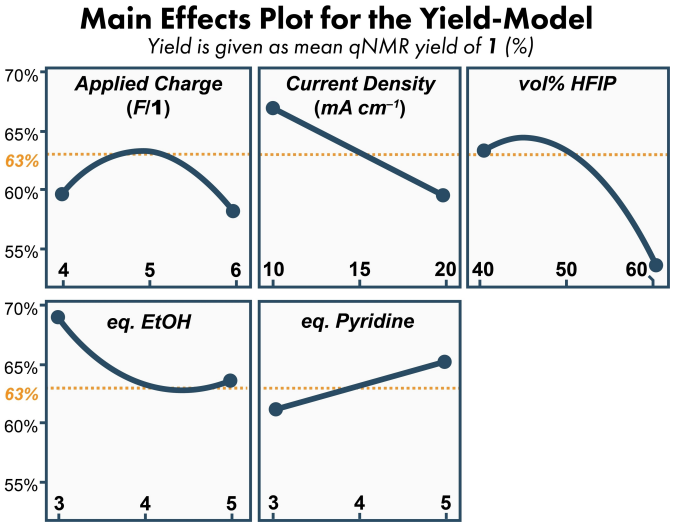

Figure 6. Main effect plot of the CCD model for the system response yield of **1**. The models overall average yield was 63 % indicated as dotted line.

A corresponding test of the smallest quadratic main effect (equivalents of ethanol) showed a linear response, contrary to the predicted quadratic behavior of the main effect. We therefore probed the model using a response optimizer algorithm (Minitab 21) to predict the reaction conditions for the maximum yield within the investigated range. Here, previously untested experimental settings were proposed for the respective effect maxima of the applied charge and the volume fraction HFIP (see Figure 6). The experimental validation revealed an offset of 17% (predicted: 77%, qNMR yield found: 60%). As the predictive power of the model inside the investigated area appeared low, the optimal experimental point was identified from the CCD, and **1** was successfully isolated in a yield of 67% (Figure 7). Further details are available in the SI.

Scope

Using the optimized reaction conditions obtained by Design of Experiments (DoE), several alcohols were tested (Figure 7).

For ethanol, product **1** was obtained in 67% isolated yield. Methanol gave **2** in 42% isolated yield. The use of isopropanol resulted in 21% isolated yield for **3**. Sulfonate **4** was synthesized in 72% isolated yield using 2-methylpropanol. 2,2-dimethylpropyl alcohol gave **5** in 62% isolated yield. Using pentanol, product **6** was isolated in a yield of 74%, which is the highest yield of all substrates.

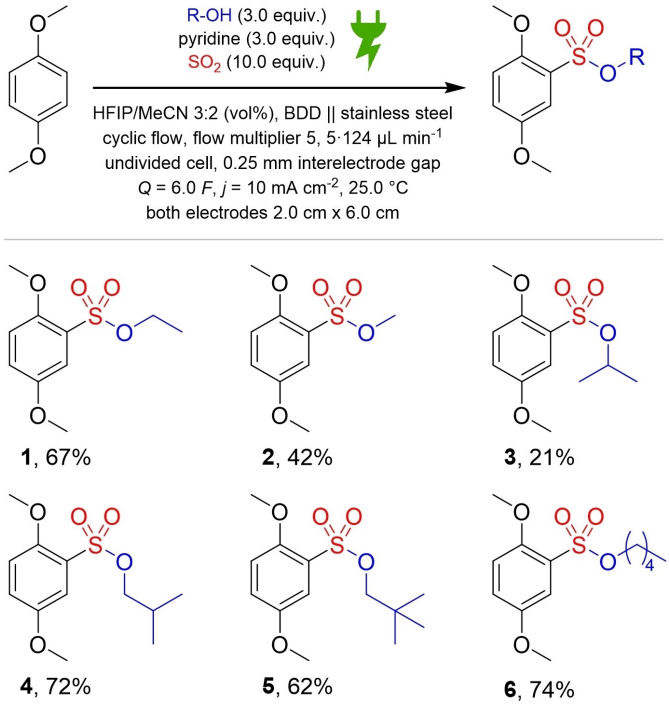

Figure 7. Scope of this electrochemical transformation with isolated yields.

Scale-Up

It's of great importance to demonstrate the robust scalability of electrochemical reactions, because this leads the way to application on industrial scale.[24] Therefore we carried out a 10-fold scale-up of the reaction depicted in in Figure 7 using pentanol as nucleophile (Table 1), since pentanol gave the highest yields of all tested alcohols (Figure 7). In this case, the isolated yield on the larger scale was 81%, which corresponds to a cell productivity of 0.6 g/h of product **6**. The space-time yield of the two cells remains nearly the same, due to the scaling factor and unchanged current density. The flow cells employed are described in Figure 8, and further details about them can be found in the Supporting Information.

Conclusions

An automated experimental setup for the electrochemical synthesis of sulfonates in a multicomponent reaction in an undivided flow cell was developed. *LABS: Laboratory Automation and Batch Scheduling*, a modular, open-source Python software developed in our group, was used to plan, and to carry out the reactions. We did show that a simple and inexpensive stock solutions of sulfur dioxide can be employed in an automated flow electrolysis setup in a concentration of up to 2.0 mol L^{-1}. Design of Experiments (DoE) was used to systemati-

Table 1. Scale-up with comparison of small cell with large flow cell.

Electrolyzer	Isolated Yield [%]	Productivity [g/h]
small flow cell	74	0.159
large modular flow cell	81	0.663

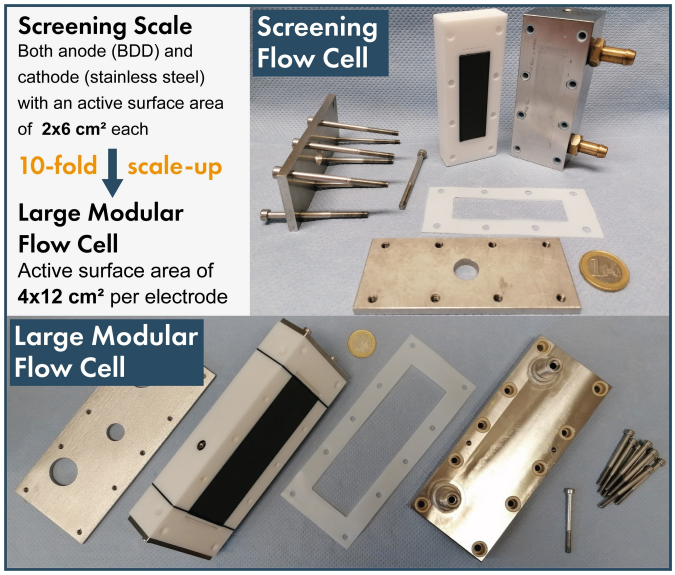

Figure 8. The two flow cells used.[25] Details can be found in the Supporting Information. Pictures by J. Schneider. The screening-scale flow cell is commercially available as "ElectraSyn flow" from IKA-Werke GmbH & CO. KG, Staufen.

cally analyze the parameters affecting the reaction, and to optimize the yield. In total, 6 examples were demonstrated with isolated yields up to 81%. The robust scalability of the electrochemical reaction was demonstrated in a 10-fold scale-up in a larger flow cell, which resulted in an increase of yield and an improved productivity. No hydrogen evolution reaction is observed during electrolysis, which could disrupt the flow setup.[26] The reaction components (HFIP, MeCN, alcohol, SO_2, and pyridine) are volatile, which simplifies reaction workup. The reaction does not require any additional supporting electrolyte, because the reaction mixture itself ensures enough conductivity. This is another example of the dual role of a supporting electrolyte as enabler of conductivity and reagent.[27]

Supporting Information

Detailed information on experimental setup, general procedures, reaction optimization, product characterization, and proposed mechanism can be found in the Supporting Information. The source code of *LABS: Laboratory Automation and Batch Scheduling* is available on GitHub under MIT license.[28] The authors have cited additional references within the Supporting Information (Ref. [29]).

Acknowledgements

We would like to thank Maurice Dörr for helpful discussions about the setup and the development of the *Eldex* pump driver and Stephan Blum for helpful discussions about electrochemical multicomponent reactions involving sulfur dioxide. Financial support by the Federal Ministry of Education and Research via the project ETOS (E-SCOPE 2.0 with number 03ZU1205LB) is acknowledged. M. M. Hielscher thanks the German Science Foundation (DFG) for the opportunity to participate in the research training group GRK2516. Open Access funding enabled and organized by Projekt DEAL.

Conflict of Interests

The authors declare no conflict of interest.

Data Availability Statement

The data that support the findings of this study are available in the supplementary material of this article.

Keywords: electrolysis · automation · design of experiments · multicomponent reactions · sulfonates

[1] a) S. Möhle, M. Zirbes, E. Rodrigo, T. Gieshoff, A. Wiebe, S. R. Waldvogel, *Angew. Chem. Int. Ed.* **2018**, *57*, 6018–6041; *Angew. Chem.* **2018**, *130*, 6124–6149; b) A. Wiebe, T. Gieshoff, S. Möhle, E. Rodrigo, M. Zirbes, S. R. Waldvogel, *Angew. Chem. Int. Ed.* **2018**, *57*, 5594–5619; *Angew. Chem.* **2018**, *130*, 5694–5721; c) M. Yan, Y. Kawamata, P. S. Baran, *Chem. Rev.* **2017**, *117*, 13230–13319; d) N. E. S. Tay, D. Lehnherr, T. Rovis, *Chem. Rev.* **2022**, *122*, 2487–2649; e) S. R. Waldvogel, B. Janza, *Angew. Chem. Int. Ed.* **2014**, *53*, 7122–7123; *Angew. Chem.* **2014**, *126*, 7248–7249; f) K. D. Moeller, *Chem. Rev.* **2018**, *118*, 4817–4833.
[2] a) J. Seidler, J. Strugatchi, T. Gärtner, S. R. Waldvogel, *MRS Energy Sustainability* **2020**, *7*, E42; b) S. O. Ganiyu, C. A. Martínez-Huitle, *Curr. Opin. Electrochem.* **2020**, *22*, 211–220.
[3] N. Sbei, T. Hardwick, N. Ahmed, *ACS Sustainable Chem. Eng.* **2021**, *9*, 6148–6169.
[4] a) D. Pollok, S. R. Waldvogel, *Chem. Sci.* **2020**, *11*, 12386–12400; b) G. Kreysa, K. Ota, R. F. Savinell, *Encyclopedia of Applied Electrochemistry*. Springer New York, New York, NY, **2014**, 964–971.
[5] S. P. Blum, D. Schollmeyer, M. Turks, S. R. Waldvogel, *Chem. Eur. J.* **2020**, *26*, 8358–8362.
[6] a) S. P. Blum, K. Hofman, G. Manolikakes, S. R. Waldvogel, *Chem. Commun.* **2021**, *57*, 8236–8249; b) N. Amri, T. Wirth, *Chem. Rec.* **2021**, *21*, 2526–2537.
[7] S. P. Blum, T. Karakaya, D. Schollmeyer, A. Klapars, S. R. Waldvogel, *Angew. Chem. Int. Ed.* **2021**, *60*, 5056–5062; *Angew. Chem.* **2021**, *133*, 5114–5120.
[8] S. P. Blum, L. Schäffer, D. Schollmeyer, S. R. Waldvogel, *Chem. Commun.* **2021**, *57*, 4775–4778.
[9] A. de A. Bartolomeu, F. A. Breitschaft, D. Schollmeyer, R. A. Pilli, S. R. Waldvogel, *Chem. Eur. J.* **2024**, *30*, e202400557.
[10] G. Laudadio, E. Barmpoutsis, C. Schotten, L. Struik, S. Govaerts, D. L. Browne, T. Noël, *J. Am. Chem. Soc.* **2019**, *141*, 5664–5668.
[11] J. Schneider, S. P. Blum, S. R. Waldvogel, *ChemElectroChem* **2023**, *10*, e202300456.
[12] a) A. Slattery, Z. Wen, P. Tenblad, J. Sanjosé-Orduna, D. Pintossi, T. den Hartog, T. Noël, *Science* **2024**, *383*, eadj1817; b) J.-M. Lu, J.-Z. Pan, Y.-M. Mo, Q. Fang, *Artificial Intelligence Chemistry* **2024**, *2*, 100057; c) N. L. Bell, F. Boser, A. Bubliauskas, D. R. Willcox, V. S. Luna, L. Cronin, *Nat. Chem. Eng.* **2024**, *1*, 180–189; d) J. Ke, C. Gao, A. A. Folgueiras-Amador, K. E. Jolley, O. de Frutos, C. Mateos, J. A. Rincón, R. C. D. Brown, M. Poliakoff, M. W. George, *Appl. Spectrosc.* **2022**, *76*, 38–50.
[13] a) L. Capaldo, Z. Wen, T. Noël, *Chem. Sci.* **2023**, *14*, 4230–4247; b) T. Noël, Y. Cao, G. Laudadio, *Acc. Chem. Res.* **2019**, *52*, 2858–2869; c) D. Pletcher, R. A. Green, R. C. D. Brown, *Chem. Rev.* **2018**, *118*, 4573–4591.
[14] M. M. Hielscher, M. Dörr, J. Schneider, S. R. Waldvogel, *Chem. Asian J.* **2023**, *18*, e202300380.
[15] C. Gütz, A. Stenglein, S. R. Waldvogel, *Org. Process Res. Dev.* **2017**, *21*, 771–778.
[16] a) M. Dörr, M. M. Hielscher, J. Proppe, S. R. Waldvogel, *ChemElectroChem* **2021**, *8*, 2621–2629; b) M. Zirbes, T. Graßl, R. Neuber, S. R. Waldvogel, *Angew. Chem. Int. Ed.* **2023**, *62*, e202219217; *Angew. Chem.* **2023**, *135*; c) S. Arndt, D. Weis, K. Donsbach, S. R. Waldvogel, *Angew. Chem. Int. Ed.* **2020**, *59*, 8036–8041; *Angew. Chem.* **2020**, *132*, 8112–8118; d) R. Möckel, E. Babaoglu, G. Hilt, *Chem. Eur. J.* **2018**, *24*, 15781–15785; e) M. Santi, J. Seitz, R. Cicala, T. Hardwick, N. Ahmed, T. Wirth, *Chem. Eur. J.* **2019**, *25*, 16230–16235.
[17] M. Selt, R. Franke, S. R. Waldvogel, *Org. Process Res. Dev.* **2020**, *24*, 2347–2355.
[18] M. B. Plutschack, B. Pieber, K. Gilmore, P. H. Seeberger, *Chem. Rev.* **2017**, *117*, 11796–11893.
[19] M. M. Hielscher, B. Gleede, S. R. Waldvogel, *Electrochim. Acta* **2021**, *368*, 137420.
[20] J. Fangmeyer, A. Behrens, B. Gleede, S. R. Waldvogel, U. Karst, *Angew. Chem. Int. Ed.* **2020**, *59*, 20428–20433; *Angew. Chem.* **2020**, *132*, 20608–20613.
[21] a) L. Schulz, S. Waldvogel, *Synlett* **2019**, *30*, 275–286; b) I. Colomer, A. E. R. Chamberlain, M. B. Haughey, T. J. Donohoe, *Nat. Chem. Rev.* **2017**, *1*, 0088; c) J. L. Röckl, D. Schollmeyer, R. Franke, S. R. Waldvogel, *Angew. Chem. Int. Ed.* **2020**, *59*, 315–319; *Angew. Chem.* **2020**, *132*, 323–327.
[22] a) D. M. Heard, A. J. J. Lennox, *Angew. Chem. Int. Ed.* **2020**, *59*, 18866–18884; b) S. Lips, S. R. Waldvogel, *ChemElectroChem* **2019**, *6*, 1649–1660; c) Y. Einaga, *Acc. Chem. Res.* **2022**, *55*, 3605–3615; d) J. V. Macpherson, *Phys. Chem. Chem. Phys.* **2015**, *17*, 2935–2949; e) S. R. Waldvogel, B. Elsler, *Electrochim. Acta* **2012**, *82*, 434–443.
[23] D. C. Montgomery, *Design and analysis of experiments*, John Wiley & Sons, Hoboken, **2020**, p. 187–200.
[24] D. Lehnherr, L. Chen, *Org. Process Res. Dev.* **2024**, *28*, 338–366.
[25] B. Gleede, M. Selt, C. Gütz, A. Stenglein, S. R. Waldvogel, *Org. Process Res. Dev.* **2020**, *24*, 1916–1926.

[26] M. Klein, S. R. Waldvogel, *Angew. Chem. Int. Ed.* **2022**, *61*, e202204140; *Angew. Chem.* **2022**, *134*, e202204140.
[27] L. G. Gombos, J. Nikl, S. R. Waldvogel, *ChemElectroChem* **2024**, *11*, e202300730 .
[28] a) Maurice Dörr, Maximilian M. Hielscher, Waldvogel-Group/LABS-DeviceDummys: Beta-Publication_submission. Reference number: 7879590, Zenodo, **2023**; b) Maurice Dörr, Maximilian M. Hielscher, Waldvogel-Group/LABS-Backend: Beta-Publication_submission. Reference number: 7879589, Zenodo, **2023**; c) Maximilian M. Hielscher, Maurice Dörr, Waldvogel-Group/LABS-Frontend: Beta-Publication_submission. Reference number: 7879586, Zenodo, **2023**.
[29] a) W. L. F. Armarego, *Purification of laboratory chemicals*, Butterworth-Heinemann is an imprint of Elsevier, Amsterdam, **2017**; b) G. Jander, K. F. Jahr, R. Martens-Menzel, L. Harwardt, H.-J. Krauss, *Massanalyse. Titrationen mit chemischen und physikalischen Indikationen*, 20. Aufl., De Gruyter, Berlin, Boston, **2022**; c) T. Rundlöf, M. Mathiasson, S. Bekiroglu, B. Hakkarainen, T. Bowden, T. Arvidsson, *J. Pharm. Biomed. Anal.* **2010**, *52*, 645–651; d) R. B. Dean, W. J. Dixon, *Anal. Chem.* **1951**, *23*, 636–638; e) J. L. Röckl, M. Dörr, S. R. Waldvogel, *ChemElectroChem* **2020**, *7*, 3686–3694.

Manuscript received: May 9, 2024
Revised manuscript received: June 19, 2024
Version of record online: August 19, 2024